QUANTIFICATION OF METAMORPHOPSIA IN CHRONIC CENTRAL SEROUS CHORIORETINOPATHY AFTER HALF-DOSE VERTEPORFIN PHOTODYNAMIC THERAPY

KYOKO FUJITA, MD, PHD,* YUTAKA IMAMURA, MD, PHD,† KEI SHINODA, MD, PHD,*‡ CELSO SOITI MATSUMOTO, MD, PHD,‡ YOSHIHIRO MIZUTANI, MD, PHD,* ATSUSHI MIZOTA, MD, PHD,‡ MITSUKO YUZAWA, MD, PHD*

Purpose: To determine the degree of metamorphopsia before and 1 year after half-dose verteporfin photodynamic therapy in eyes with chronic central serous chorioretinopathy.

Methods: This was a retrospective, noncomparative, interventional case series. Forty-five eyes of 45 consecutive patients with chronic central serous chorioretinopathy were evaluated. The degree of metamorphopsia was measured with M-CHARTS before and at 1, 3, 6, 9, and 12 months after half-dose verteporfin photodynamic therapy. The best-corrected visual acuity was also measured.

Results: Forty of the 45 eyes had a complete resolution of the serous retinal detachment at 1 month, 1 eye at 3 months, and 3 eyes at 6 months. The serous retinal detachment in one eye persisted throughout the follow-up period. The mean horizontal metamorphopsia score improved significantly from 0.61 ± 0.52° at baseline to 0.49 ± 0.56° at 12 months (P = 0.04). The vertical metamorphopsia score improved significantly from 0.52 ± 0.53° at baseline to 0.33 ± 0.46° at 12 months (P = 0.005).

Conclusion: Half-dose verteporfin photodynamic therapy for chronic central serous chorioretinopathy results in significant improvements of metamorphopsia at 1 year, especially in eyes with good best-corrected visual acuity at the baseline. Half-dose verteporfin photodynamic therapy can be a therapeutic option for patients with good visual acuity who complain of metamorphopsia.

RETINA 34:964–970, 2014

Central serous chorioretinopathy (CSC) is characterized by a serous retinal detachment (SRD) in the macular area.[1] Although CSC has been described as a benign and self-limiting disease, a persistent SRD can lead to poor vision and foveal atrophy. The foveal atrophy is most likely because of photoreceptor and retinal pigment epithelium damage that is caused by the prolonged separation of the photoreceptors from the retinal pigment epithelium.[2–4]

Photodynamic therapy (PDT) has been reported to enhance the absorption of fluid from the subretinal space in eyes with CSC by remodeling the structures of the choroidal vasculature. The remodeling causes alterations in the choroidal vascular hyperpermeability.[5] Several studies have reported favorable outcomes after PDT.[6–8] In addition, the safety and beneficial effects of "safety-enhanced" half-dose verteporfin (Visudyne; Novartis AG, Bulach, Switzerland) PDT have been demonstrated for both acute and chronic CSC.[9–11] However, there are patients who still complain of metamorphopsia even after a complete resolution of the SRD.

Amsler charts are widely used to detect metamorphopsia.[12] The Amsler chart is a useful method to establish the presence of metamorphopsia, but it does not allow a quantification of the degree of metamorphopsia and is therefore difficult to use for follow-up studies. Matsumoto et al have developed a new metamorphopsia chart called M-CHARTS (Inami Co, Tokyo, Japan) to evaluate the degree of metamorphopsia quantitatively (Figure 1).[13–17]

The purpose of this study was to determine the degree of metamorphopsia by the M-CHARTS before and after

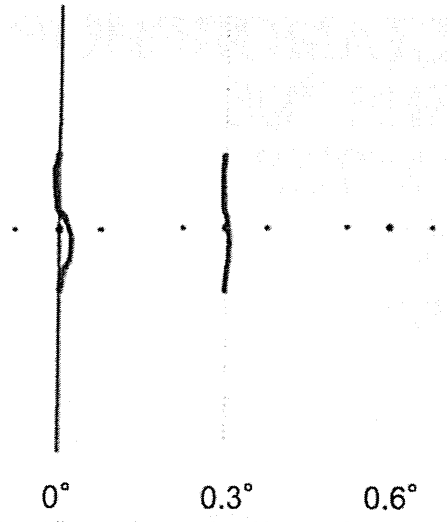

Fig. 1. Dotted lines are shown to the subject one after another, until the subject reports that the line is straight. In this case, the vertical solid line was distorted at 0.3°, after lines with larger dot intervals were recognized as less distorted. Line 0.6° was recognized as straight, thus the MV score is 0.6°.

half-dose verteporfin PDT in patients with chronic CSC. In addition, the relationship between the metamorphopsia and the integrity of the microstructures of the photoreceptors at the macula was evaluated.

Patients and Methods

We studied a series of consecutive patients who had undergone half-dose verteporfin PDT for chronic CSC between November 2009 and March 2011 and were followed for at least 12 months after the PDT. All of the patients had a history of CSC characterized by visual disturbances persisting for more than 6 months or had a recurrent history of CSC. The inclusion criteria were presence of leakage and multifocal or diffuse retinal pigment epithelium decompensation on fluorescein angiography, choroidal vascular hyperpermeability, and abnormal dilatation of the choroidal vasculature on indocyanine green angiography. In addition, all of the eyes had a SRD that overlapped the fovea. Eyes that had been treated with laser photocoagulation and those with recurrent CSC were included. The exclusion criteria were severely myopic or hyperopic eyes with refractive errors (spherical equivalent) of more than 6 diopters, had evidence of choroidal neovascularization, presence of any other ocular diseases that could affect the visual acuity, and presence of media opacities such as cataracts that could interfere with obtaining high quality optical coherence tomographic images, fluorescein angiography, and indocyanine green angiography images. Eyes with a decimal best-corrected visual acuity (BCVA) of <0.1 (Snellen equivalent of 20/200) were excluded because the limit of the decimal BCVA that M-CHARTS could detect metamorphopsia has been reported to be 0.1.[14]

All the patients completed the 12 months of follow-up examinations. The examinations included dilated fundus examination, measurement of the BCVA, and OCT (Spectralis HRA + OCT; Heidelberg Engineering GmbH, Heidelberg, Germany) scanning at the baseline and at 1, 3, 6, 9, and 12 months after the half-dose verteporfin PDT.

We used the M-CHARTS to quantify the degree of metamorphopsia. This chart is based on the fact that patients with metamorphopsia perceive a straight line as a curved or an irregular line.[14,15] When the straight line is replaced with a dotted line and the dot interval is changed from fine to coarse, the distortion of the line decreases with increasing dot intervals until the dotted line appears straight. The M-CHARTS was designed based on this, and 1 set consisted of 19 charts with each chart having a dotted line of different dot intervals. The angular separation of the dots ranged from 0.2° to 2.0°. The examination distance was 30 cm, and the refraction of the eye was adjusted to this distance. In the M-CHARTS test, a vertical straight line (0°) was first shown to the patient, and if the patient reported the straight line as being straight, the metamorphopsia score was 0°. If the patient reported the straight line as distorted, the next chart with a greater separation of the dots was shown. The dot intervals changed from fine to coarse, and the charts were shown one after another until the patient reported perceiving the dotted line as being straight. The visual angle that was reported to be straight was considered to be the M-CHARTS score. The M-CHARTS score was determined for both vertical and horizontal lines (Figure 1).

To reduce the test variations, both vertical and horizontal tests were repeated at least two times for each subject, and the average of the two test scores was used. An M-CHARTS score >0.2° was defined as a positive detection of metamorphopsia.

From the *Department of Ophthalmology, Surugadai Nihon University Hospital, Tokyo, Japan; †Department of Ophthalmology, Teikyo University School of Medicine, University Hospital Mizonokuchi, Kawasaki-shi, Japan; and ‡Department of Ophthalmology, Teikyo University School of Medicine, University Hospital Itabashi, Tokyo, Japan.

Supported by Researches on Sensory and Communicative Disorders from the Ministry of Health, Labor, and Welfare, Japan.

None of the authors have any conflicting interests to disclose.

Reprint requests: Kei Shinoda, MD, PhD, Department of Ophthalmology, Teikyo University School of Medicine, Kaga 2-11-1, Itabashi-ku, Tokyo 173-8606, Japan; e-mail: shinodak@med.teikyo-u.ac.jp

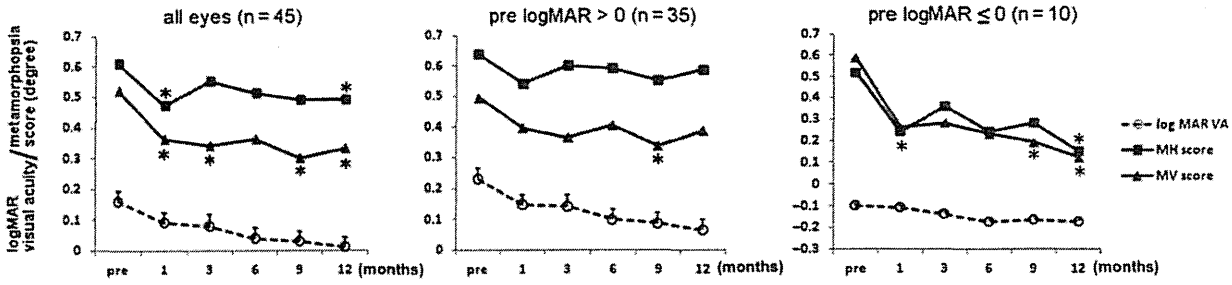

Fig. 2. Changes of the mean metamorphopsia score and mean best-corrected visual acuity before and after half-dose photodynamic therapy for chronic central serous chorioretinopathy. Left: The horizontal metamorphopsia (MH) and vertical metamorphopsia (MV) scores for all eyes. Significant improvements were observed in the MH scores at 1 and 12 months and in the MV scores at 1, 3, 9, and 12 months compared with the baseline scores. Middle: Comparison of the metamorphopsia scores and BCVA before and after half-dose photodynamic therapy for chronic central serous chorioretinopathy in eyes with decimal BCVA <1.0 (Group B). Significant improvement was not observed at all follow-up times for both the MH and MV scores except at 9 months in the MV score compared with the baseline scores. Right: Comparison of the metamorphopsia scores and BCVAs before and after half-dose photodynamic therapy for chronic central serous chorioretinopathy in eyes with decimal BCVA ≥1.0 at baseline (Group A). Significant improvement was observed at 12 months in the MH score and at 1, 9, 12 months in the MV score comparing with the baseline scores. *$P < 0.05$.

Spectral domain optical coherence tomographic images were recorded from a 9 × 9 mm area centered on the fovea. Horizontal and vertical scans through the fovea were recorded for each eye. The status of the photoreceptor inner/outer segment (IS/OS) line and the cone outer segment tips (COST) line at 12 months was classified as follows: eyes with an intact IS/OS line in both horizontal and vertical scans were classified as having an intact IS/OS line, and eyes in which the IS/OS line was not detected in at least 1 scan was classified as an absent IS/OS line. Each eye also was classified based on the status of the COST line beneath the macula using the same criteria described for the IS/OS line. The morphologic changes of the macular photoreceptor microstructures were evaluated by two masked investigators (K.F. and Y.M.) independently.

Photodynamic therapy was performed using half-dose verteporfin. For this, 3 mg/m^2 body size of verteporfin was infused intravenously more than 10 minutes, and 15 minutes after beginning the infusion, the laser treatment was begun. The total light energy delivered to the area of hyperpermeability detected on the indocyanine green angiography images was 50 J/cm^2. The spot size covered the areas with choroidal hyperpermeability on the indocyanine green angiography.

The study protocol was approved by the Ethics Committee of the Surugadai Nihon University Hospital, and a written informed consent was obtained from all patients. All experiments were performed in accordance with the Declaration of Helsinki for research involving human subjects.

The BCVA was measured with Landolt charts, and the decimal values were converted to logarithm of the minimum angle of resolution (logMAR) units. Student *t*-tests were used to assess the significance of the changes in the BCVA, and the Wilcoxon signed-rank tests were used to assess the changes of the metamorphopsia scores. For comparisons between 2 groups that were classified according to the baseline BCVA, that is, those with BCVA ≥1.0 (Snellen equivalent of 20/20) or <1.0 (20/20), we used the Wilcoxon signed-rank tests. Mann–Whitney *U* tests were used to compare the horizontal metamorphopsia (MH) and vertical metamorphopsia (MV) scores between presence or absence of the IS/OS line and COST line at 12 months. A $P < 0.05$ was taken to be statistically significant. The analyses were performed using StatView version 5.0 (SAS Inc, Cary, NC).

Results

Forty-five eyes of 45 consecutive patients met the inclusion criteria for this study. The mean age of the 45 patients with chronic CSC was 53.0 ± 9.7 years (range, 36–75 years) and consisted of 43 men and 2 women. Although all patients either stopped or did not have a history of corticosteroid use before the half-dose verteporfin PDT, one patient had used corticosteroid cream for the skin for at least 1 year. The mean duration of the symptom before treatment was 49 months (range, 6–240 months). All patients met each scheduled follow-up visit and underwent all examinations.

The SRD was resolved at 1 month in 40 eyes, at 3 months in 1 eye, and at 6 months in 3 eyes. One eye had a persistent SRD throughout the follow-up period. We did not repeat the PDT in this patient because the macula was already atrophic, and we believed that the BCVA would not improve. During the follow-up period of 1 year, a recurrence of the SRD occurred in 2 eyes. In 1 eye, the SRD was absorbed in 6 months but recurred at 9 months This SRD was spontaneously resorbed at 14 months. In the other eye, the SRD was resorbed in 1 month and recurred at 6 months. The

SRD persisted, and 24 months later, PDT was successfully performed to resolve the SRD. No side effects due to half-dose verteporfin PDT were observed in all the cases.

The patients' postoperative BCVA ranged from 0.15 to 1.5 (from 20/130 to 20/13). Therefore, M-CHARTS examination was performed on all patients. The mean baseline BCVA was 0.16 ± 0.23 logMAR units (equivalent to 20/100), and there was a significant improvement to 0.09 ± 0.22 at 1 month, 0.08 ± 0.24 at 3 months, 0.04 ± 0.22 at 6 months, 0.03 ± 0.22 at 9 months, and 0.01 ± 0.23 logMAR units at 12 months (20/25, 20/24, 20/22, 20/21, and 20/20, respectively; $P < 0.05$ for all comparisons, paired t-tests).

Eighteen of 45 eyes had an improvement of the MH score ≥0.2°, 19 eyes had no change, and 8 eyes had a worse score at 12 months. Twenty-one of 45 eyes had an improvement in the MV score of ≥0.2°, 18 eyes had no change, and 6 eyes had a worse score. The mean MH score was 0.61 ± 0.52° at the baseline, 0.47 ± 0.53° at 1 month, 0.55 ± 0.49° at 3 months, 0.51 ± 0.52° at 6 months, 0.49 ± 0.45° at 9 months, and 0.49 ± 0.56° at 12 months (Figure 2). The mean MH score did not improve significantly at 3, 6, and 9 months ($P > 0.05$, Wilcoxon signed-rank test), but it improved significantly between the baseline and 1 and 12 months ($P < 0.05$, Wilcoxon signed-rank test).

The mean MV scores in degrees were 0.52 ± 0.53° at the baseline, 0.36 ± 0.31° at 1 month, 0.34 ± 0.34° at 1 month, 0.36 ± 0.43° at 6 months, 0.30 ± 0.37° at 9 months, and 0.33 ± 0.46° at 12 months. The mean MV scores improved significantly at 1, 3, 9, and 12 months compared with the baseline score ($P < 0.05$, Wilcoxon signed-rank test) but did not improve

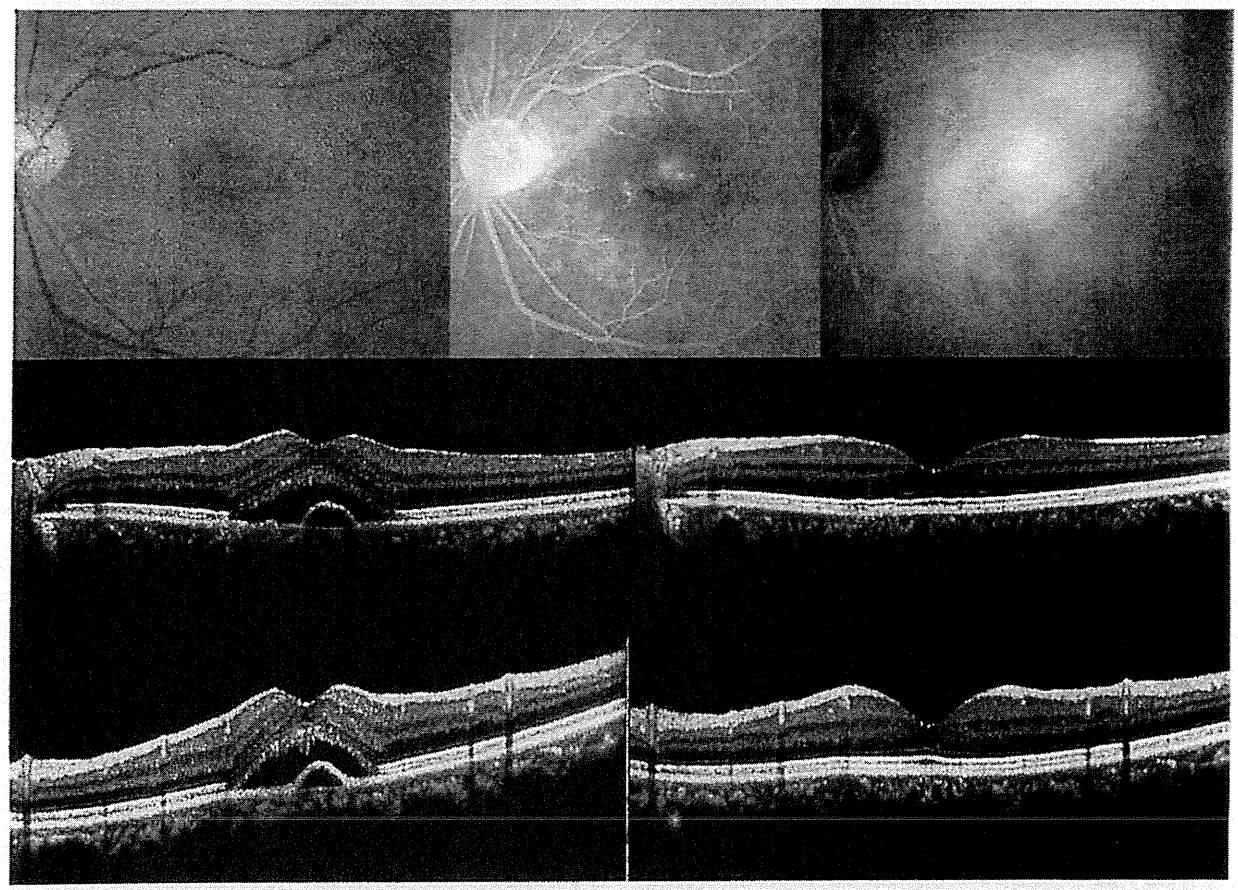

Fig. 3. Representative case from Group A that had an improvement in the metamorphopsia score after half-dose verteporfin photodynamic therapy. A 57-year-old man with chronic central serous chorioretinopathy with a baseline decimal visual acuity of 1.2. Upper left: His MH score and MV score at baseline were 0.9° and 1.0°, respectively. Both scores were improved to 0° at 12 months. Baseline color fundus photograph showing SRD at the macular area including pigment epithelial detachment (PED). Upper middle: Baseline fluorescein angiography showed some focal leakage at the macula. Upper right: Baseline indocyanine green angiography showing choroidal hyperpermeability at the macula. Middle left: Baseline spectral domain optical coherence tomographic (SD-OCT) image of horizontal scan through the fovea showing the SRD and PED. Middle right: SD-OCT image of horizontal scan through the fovea obtained at 12 months showing complete resolution of the SRD and PED. Bottom left: Baseline SD-OCT image of vertical scan through the fovea showed SRD and PED. Bottom right: SD-OCT image of vertical scan through the fovea obtained at 12 months showing complete resolution of the SRD and PED.

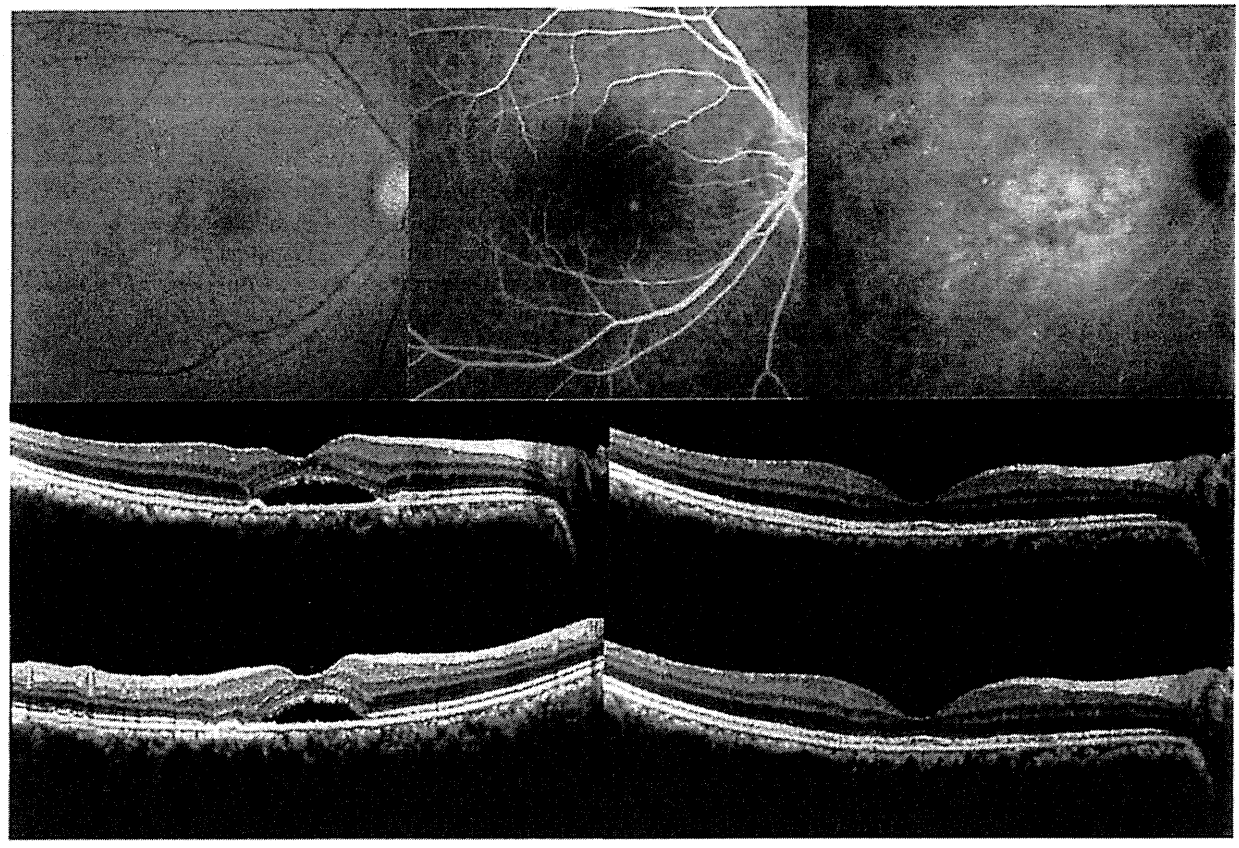

Fig. 4. Representative case from Group B. A 61-year-old woman with chronic central serous chorioretinopathy. Her visual acuity at baseline was 0.5, and her horizontal metamorphopsia (MH) and vertical metamorphopsia (MV) score at baseline were 0.4° and 0.5°, respectively. At 12 months, MH score and MV score were 0.5° and 0.6°, respectively. Upper left: Baseline color fundus photograph showing a serous retinal detachment (SRD) at the macular area. Upper middle: Baseline fluorescein angiography showed some focal leakage at the macula. Upper right: Baseline indocyanine green angiography showed choroidal hyperpermeability at the macula. Middle left: Baseline spectral domain optical coherence tomography (SD-OCT) image of horizontal scan through the fovea showed SRD. Middle right: SD-OCT image of horizontal scan through the fovea obtained at 12 months showing complete resolution of the SRD. Bottom left: Baseline SD-OCT image of vertical scan through the fovea showed SRD. Bottom right: SD-OCT image of vertical scan through the fovea obtained at 12 months showing complete resolution of the SRD.

significantly at 6 months ($P > 0.05$, Wilcoxon signed-rank test; Figures 2 and 3).

We divided the eyes according to the BCVA at baseline; there were 10 eyes with a BCVA of ≤0 logMAR units (Group A) and 35 eyes with a BCVA of >0 logMAR units (Group B). In Group A, the mean MH scores improved significantly from 0.52 ± 0.53° to 0.15 ± 0.25° ($P = 0.04$, Wilcoxon signed-rank test), and the mean MV score improved significantly from 0.59 ± 0.59° to 0.12 ± 0.21° at 12 months ($P = 0.04$, Wilcoxon signed-rank test) compared with that at the baseline (Figures 2 and 3). In Group B, neither the mean MH scores (from 0.64 ± 0.52° to 0.59 ± 0.59°, $P > 0.05$, Wilcoxon signed-rank test) nor the mean MV scores (from 0.49 ± 0.52° to 0.38 ± 0.50°) improved significantly ($P > 0.05$, Wilcoxon signed-rank test; Figures 2 and 4).

The spectral domain optical coherence tomographic images showed that 36 eyes had an intact IS/OS line, and 17 eyes had an intact COST line at 12 months (Table 1). The BCVA was significantly higher in eyes with an intact IS/OS line (n = 36) than in eyes without it (n = 9; $P = 0.0002$, t-test) and also significantly higher in eyes with an intact COST line (n = 17) than in eyes without it (n = 26; $P = 0.001$, t-test). The MH and MV scores were not significantly different between eyes with (n = 36) and without (n = 9) an intact IS/OS line ($P > 0.05$, for both comparisons, Mann–Whitney U test). The MH and MV sores were not significantly different between eyes with (n = 17) and without (n = 28) an intact COST line ($P > 0.05$, for both comparisons, Mann–Whitney U test).

Discussion

Our findings showed that both the MV score and the MH score were significantly improved at 12 months

Table 1. Comparisons of Visual Acuity, Horizontal, and Vertical Metamorphopsia Scores Between Eyes With and Without the IS/OS Junction and the COST Lines at 12 Months After Half-Dose PDT

	IS/OS			COST		
	Present (n = 36)	Absent (n = 9)	P*	Present (n = 17)	Absent (n = 28)	P*
LogMAR VA: min–max (mean ± SD)	−0.17 to 0.39 (−0.06 ± 0.15)	−0.07 to 0.69 (0.30 ± 0.27)	0.0002	−0.17 to 0.04 (−0.13 ± 0.07)	−0.17 to 0.69 (0.09 ± 0.25)	0.001
Snellen VA: min–max (mean)	20/50 to 20/13 (20/17)	20/100 to 20/17 (20/40)		20/22 to 20/13 (20/15)	20/100 to 20/13 (20/25)	
MH score: min–max (median)	0 to 2.0 (0.35)	0 to 1.9 (0.60)	0.357	0 to 2.0 (0.30)	0 to 1.9 (0.50)	0.372
MV score: min–max (median)	0 to 2.0 (0.10)	0 to 2.0 (0.40)	0.75	0 to 2.0 (0.20)	0 to 2.0 (0.10)	0.774

LogMAR VA, logarithm of minimal angle resolution visual acuity; SD, standard deviation; min, minimum; max, maximum.
*Statistical comparison was made using Student *t*-test for logMAR VA and Mann–Whitney *U* test for MH and MV scores.

after the half-dose verteporfin PDT for eyes with chronic CSC. For eyes whose baseline decimal BCVA was ≧1.0, both the MV and MH scores improved significantly after the PDT. The presence of the IS/OS line and COST line at 12 months was significantly correlated with the improvement of BCVA, but it was not significantly correlated with the MH or MV scores.

Photodynamic therapy with verteporfin has been shown to improve the visual acuity and reduce the subretinal fluid in eyes with chronic CSC.[6–9,11] Despite the anatomical success and improvement of the visual acuity, patients often complain of metamorphopsia as seen in eyes after successful removal of the epiretinal membrane.[18]

Metamorphopsia has been suggested to result from a displacement of the photoreceptors and a false localization of the image seen by these displaced photoreceptors.[12] The mechanism of metamorphopsia in CSC has not been definitively determined, but a possible explanation is that the regular intervals between adjacent photoreceptors are disrupted by the subretinal fluid. We found that the correlations between the integrity of the IS/OS line and the COST line and the metamorphopsia score were not significant. Ooto et al[19] reported that the adaptive optics scanning laser ophthalmoscope images showed abnormal cone mosaic patterns and reduced cone densities in eyes with resolved CSCs. It is highly likely that three-dimensional alterations of the photoreceptors would not be visible in the images obtained by the spectral domain optical coherence tomography that we used.

Our findings, that eyes with a significant improvement of the mean horizontal and vertical metamorphosia scores at 12 months had baseline decimal BCVA of ≧1.0, suggest that an earlier intervention by PDT would be better. Most published studies suggest that PDT with verteporfin is a safe and efficacious treatment in CSC and that complications are rare, especially when total energy delivered to the retina is reduced.[9–11]

This study has several limitations. This was a retrospective study with no control group. In addition, the number of patients was relatively small. Therefore, further studies with larger sample sizes are needed to confirm these results.

In conclusion, half-dose verteporfin PDT for chronic CSC resulted in significant improvements of the metamorphosia score at 12 months. The improvements of both the MH and MV were significant in eyes with BCVA 1.0. We conclude that the use of M-CHARTS is a useful way to quantify metamorphopsia in CSC undergoing half-dose verteporfin PDT. We recommend half-dose verteporfin PDT for patients with CSC of good vision, particularly when metamorphopsia is present.

Key words: metamorphopsia, M-CHARTS, optical coherence tomography, photodynamic therapy, chronic central serous chorioretinopathy.

References

1. Gass JD. Pathogenesis of disciform detachment of the neuroepithelium. Am J Ophthalmol 1967;63(suppl):1–139.
2. Wang MS, Sander B, Larsen M. Retinal atrophy in idiopathic central serous chorioretinopathy. Am J Ophthalmol 2002;133: 787–793.
3. Piccolino FC, de la Longrais RR, Ravera G, et al. The foveal photoreceptor layer and visual acuity loss in central serous chorioretinopathy. Am J Ophthalmol 2005;139:87–99.
4. Imamura Y, Fujiwara T, Spaide RF. Fundus autofluorescence and visual acuity in central serous chorioretinopathy. Ophthalmology 2011;118:700–705.
5. Chan WM, Lam DS, Lai TY, et al. Choroidal vascular remodeling in central serous chorioretinopathy after indocyanine green angiography guided photodynamic therapy with verteporfin: a novel treatment at the primary disease level. Br J Ophthalmol 2003;87:1453–1458.
6. Cardillo Piccolino F, Eandi CM, Ventre L, et al. Photodynamic therapy for chronic central serous chorioretinopathy. Retina 2003;23:752–763.
7. Yannuzzi LA, Slakter JS, Gross NE, et al. Indocyanine green angiography guided photodynamic therapy for treatment of chronic central serous chorioretinopathy: a pilot study. Retina 2003;23:288–298.
8. Taban M, Boyer DS, Thomas EL, Taban M. Chronic central serous chorioretinopathy: photodynamic therapy. Am J Ophthalmol 2004;137:1073–1080.
9. Lai TY, Chan WM, Li H, et al. Safety enhanced photodynamic therapy with half dose verteporfin for chronic central serous chorioretinopathy: a short-term pilot study. Br J Ophthalmol 2006;90:869–874.
10. Chan WM, Lai TY, Lai RY, et al. Half dose verteporfin photodynamic therapy for acute central serous chorioretinopathy. Ophthalmology 2008;115:1756–1765.
11. Chan WM, Lai TY, Lai RY, et al. Safety enhanced photodynamic therapy for chronic central serous chorioretinopathy. Retina 2008;28:85–93.
12. Amsler M. Earliest symptoms of diseases of the macula. Br J Ophthalmol 1953;37:521–537.
13. Matsumoto C, Arimura E, Hashimoto S, et al. A new method for quantification of metamorphopsia using M-CHARTS. Rinsho Ganka 2000;54:373–377.
14. Matsumoto C, Arimura E, Okuyama S, et al. Quantification of metamorphopsia in patients with epiretinal membranes. Invest Ophthalmol Vis Sci 2003;44:4012–4016.
15. Arimura E, Matsumoto C, Okuyama S, et al. Retinal contraction and metamorphopsia scores in eyes with idiopathic epiretinal membrane. Invest Ophthalmol Vis Sci 2005;46: 2961–2966.
16. Arimura E, Matsumoto C, Okuyama S, et al. Quantification of metamorphopsia in a macular hole patient using M-CHARTS. Acta Ophthalmol Scand 2007;85:55–59.
17. Kinoshita T, Imaizumi H, Okushiba U, et al. Time course of changes in metamorphopsia, visual acuity, and OCT parameters after successful epiretinal membrane surgery. Invest Ophthalmol Vis Sci 2012;53:3592–3597.
18. Okamoto F, Okamoto Y, Hiraoka T, Oshika T. Effect of vitrectomy for epiretinal membrane on visual function and vision-related quality of life. Am J Ophthalmol 2009;147: 869–874.
19. Ooto S, Hangai M, Sakamoto A, et al. High-resolution imaging of resolved central serous chorioretinopathy using adaptive optics scanning laser ophthalmoscopy. Ophthalmology 2010; 117:1800–1809.

Jpn J Ophthalmol
DOI 10.1007/s10384-013-0300-6

THE OFFICIAL INTERNATIONAL JOURNAL OF THE JAPANESE OPHTHALMOLOGICAL SOCIETY

CLINICAL INVESTIGATION

Autoantibodies to transient receptor potential cation channel, subfamily M, member 1 in a Japanese patient with melanoma-associated retinopathy

Yukiko Morita · Kazuhiro Kimura · Youichiro Fujitsu · Atsushi Enomoto · Shinji Ueno · Mineo Kondo · Koh-Hei Sonoda

Received: 23 May 2013 / Accepted: 3 December 2013

Abstract
Purpose To report a case of melanoma-associated retinopathy (MAR) in a Japanese patient found to have autoantibodies to transient receptor potential cation channel, subfamily M, member 1 (TRPM1).
Case An 82-year-old man presented with blurred vision OS as well as night blindness and photopsia OU. Fundus photography, fluorescein angiography, and spectral domain-optical coherence tomography findings were essentially normal. Goldmann perimetry revealed a relative central scotoma, including the blind spot in the right eye, as well as a relative scotoma around a blind spot OS. The full-field scotopic electroretinograms showed a "negative-type" pattern OU, suggestive of extensive bipolar cell dysfunction. Systemic examination revealed that the patient had malignant melanoma of the anus with lung metastasis. Autoantibodies to TRPM1 were detected in the serum of the patient by immunoblot analysis. Vitreous opacity developed during follow-up. The visual symptoms and vitreous opacity of the patient were markedly improved after oral prednisolone therapy. The patient died as a result of widespread metastasis of the melanoma at 11 months after his first visit.
Conclusion The present case is the first reported instance of MAR positive for autoantibodies to TRPM1 in an Asian patient.

Keywords Melanoma-associated retinopathy · Electroretinogram (ERG) · Transient receptor potential cation channel, subfamily M, member 1 (TRPM1) · Paraneoplastic retinopathy

Y. Morita · K. Kimura (✉) · Y. Fujitsu · K.-H. Sonoda
Department of Ophthalmology, Yamaguchi University Graduate School of Medicine, 1-1-1 Minami-Kogushi, Ube, Yamaguchi 755-8505, Japan
e-mail: k.kimura@yamaguchi-u.ac.jp

A. Enomoto
Department of Pathology, Nagoya University Graduate School of Medicine, Nagoya, Japan

S. Ueno
Department of Ophthalmology, Nagoya University Graduate School of Medicine, Nagoya, Japan

M. Kondo
Department of Ophthalmology, Mie University Graduate School of Medicine, Tsu, Japan

Introduction

Melanoma-associated retinopathy (MAR) is a paraneoplastic autoimmune manifestation of melanoma that is characterized by various visual signs and symptoms including night blindness, photopsia, visual field defects, and abnormal color vision [1–8]. Patients with MAR also have characteristic electroretinograms (ERGs). The scotopic full-field ERG elicited by a bright flash stimulus shows a "negative-type" pattern with an a-wave of normal amplitude and a b-wave smaller than the a-wave [1–6], suggesting that in MAR patients, the retinal bipolar cells are affected. Historically, autoantibodies to bipolar cells have been recognized as markers of MAR, but the specific bipolar cell antigen has not been identified [8–12].

We and others recently identified autoantibodies specific for transient receptor potential cation channel, subfamily M, member 1 (TRPM1) in the serum of MAR patients [13, 14]. TRPM1 is specifically expressed in retinal ON bipolar cells and functions as a component of the transduction channel in these cells [15–17]. All four MAR

Published online: 29 January 2014

patients with autoantibodies to TRPM1 in these previous reports were Caucasian [13, 14], and individuals with TRPM1-related MAR have not been described for other ethnic groups. Malignant melanoma is rare in the Japanese population, with a prevalence of only 0.002 %, compared with a frequency of 0.015 % in white populations.

We now report a case of MAR positive for serum autoantibodies to TRPM1 in a Japanese individual with melanoma of the anus and metastasis to the lung.

Case report

An 82-year-old man visited Yamaguchi University Hospital with complaints of blurred vision OS as well as night blindness and photopsia OU with a duration of about 1 month. He had not recently been diagnosed with any ocular or systemic disease, including any malignant tumors. His family history revealed no members with any eye diseases. Our initial examination found that his best corrected visual acuity (BCVA) was 1.2 OD and 0.6 OS. Slit-lamp assessment, intraocular pressure measurement, fundus examination, and fluorescein angiography findings were essentially normal OU (Fig. 1a, b). Spectral domain-optical coherence tomography (SD-OCT) (Cirrus HD-OCT; Carl Zeiss Meditec, Dublin, CA, USA) revealed a normal macular structure, with the exception of a slight irregularity of the retinal pigment epithelium in both eyes (Fig. 1c). The thickness of the parafoveal nasal inner nuclear layer (INL) was 40 μm OD and 36 μm OS. Given that the normal thickness of the parafoveal nasal INL was previously determined to be ~40 μm [18], there did not appear to be any thinning of the INL in this patient.

Goldmann perimetry revealed that the visual fields manifested general depression OU. A relative central scotoma including a blind spot was detected OD, and a relative scotoma around the blind spot was detected OS, with the I-4e target (Fig. 2a). Color vision tested with Ishihara color plates was normal, but the Standard Pseudoisochromatic Plates part 2 (SPP-2) test and the panel D-15 test revealed a mild blue-yellow defect OS. A dark-adaptation test revealed a poorly defined red-cone break and elevated threshold level, with a log threshold (arbitrary units) value of 6 after 40 min. Full-field ERGs were recorded with a bright flash stimulus of 20 J after 20 min of dark adaptation. They showed a normal a-wave and a b-wave with a markedly reduced amplitude, giving rise to a "negative-type" pattern OU (Fig. 2b).

On the basis of these ophthalmological and electrophysiological findings, we tentatively diagnosed the patient with paraneoplastic retinopathy and performed systemic examinations. Whole-body computed tomography (CT) revealed a tumor in his right lung (Fig. 2c). Biopsy specimens were obtained from a hilar lymph node in the right lung by bronchoscopy, and histology revealed the mass to be a malignant melanoma (Fig. 2d). Positron emission tomography was performed, but the site of the primary tumor was not identified. There was physiological accumulation of the tracer in the bladder. We consulted a dermatologist, and the patient was then treated with DAV-Feron (dacarbazine, nimustine hydrochloride, vincristine, and interferon-β) chemotherapy. His BCVA remained at 1.0 OD and 0.7 OS, but vitreous opacity appeared OS and perimetry revealed enlarged blind spots OU.

Given that autoantibodies to TRPM1 have been detected in patients with paraneoplastic retinopathy associated with dysfunction of retinal ON bipolar cells [13, 14], we examined whether such autoantibodies were also present in the serum of our MAR patient. Immunoblot analysis revealed that serum from the patient yielded a pronounced immunoreactive band with lysates of cells transfected with an expression vector for human TRPM1 (Fig. 3). Negative control serum did not show such reactivity. These results suggested that the serum of the proband contained autoantibodies to TRPM1.

The patient received oral prednisolone at 40 mg/day for treatment of his MAR. Four weeks after the onset of prednisolone therapy, the vitreous opacity had disappeared and the blind spot enlargement was markedly attenuated OU. Four months after his initial visit, the patient was diagnosed with anal malignant melanoma, with the late diagnosis being attributable to the misidentification of his anal tumor as a hemorrhoid. The lung tumor was thus likely a metastasis from anal malignant melanoma. The patient died at 11 months after his first visit as a result of metastasis to the brain, lung, liver, bilateral hilar lymph nodes, mediastinal lymph nodes, and inguinal lymph nodes.

Discussion

The patient presented with blurred vision, night blindness, and photopsia associated with a "negative-type" ERG, indicative of dysfunction of retinal bipolar cells. Systemic examination revealed malignant melanoma in the lung and anus. The serum of the patient was also positive for autoantibodies to TRPM1. On the basis of these findings, we diagnosed the patient with MAR likely caused by autoantibodies to TRPM1. Only four patients with TRPM1-related MAR have been reported to date, all of whom were Caucasian [13, 14]. The present Japanese patient thus represents the first case of TRPM1-related MAR in an ethnic group other than Caucasian. Our findings suggest that autoantibodies to TRPM1 may play an important role in the pathogenesis of MAR regardless of ethnicity.

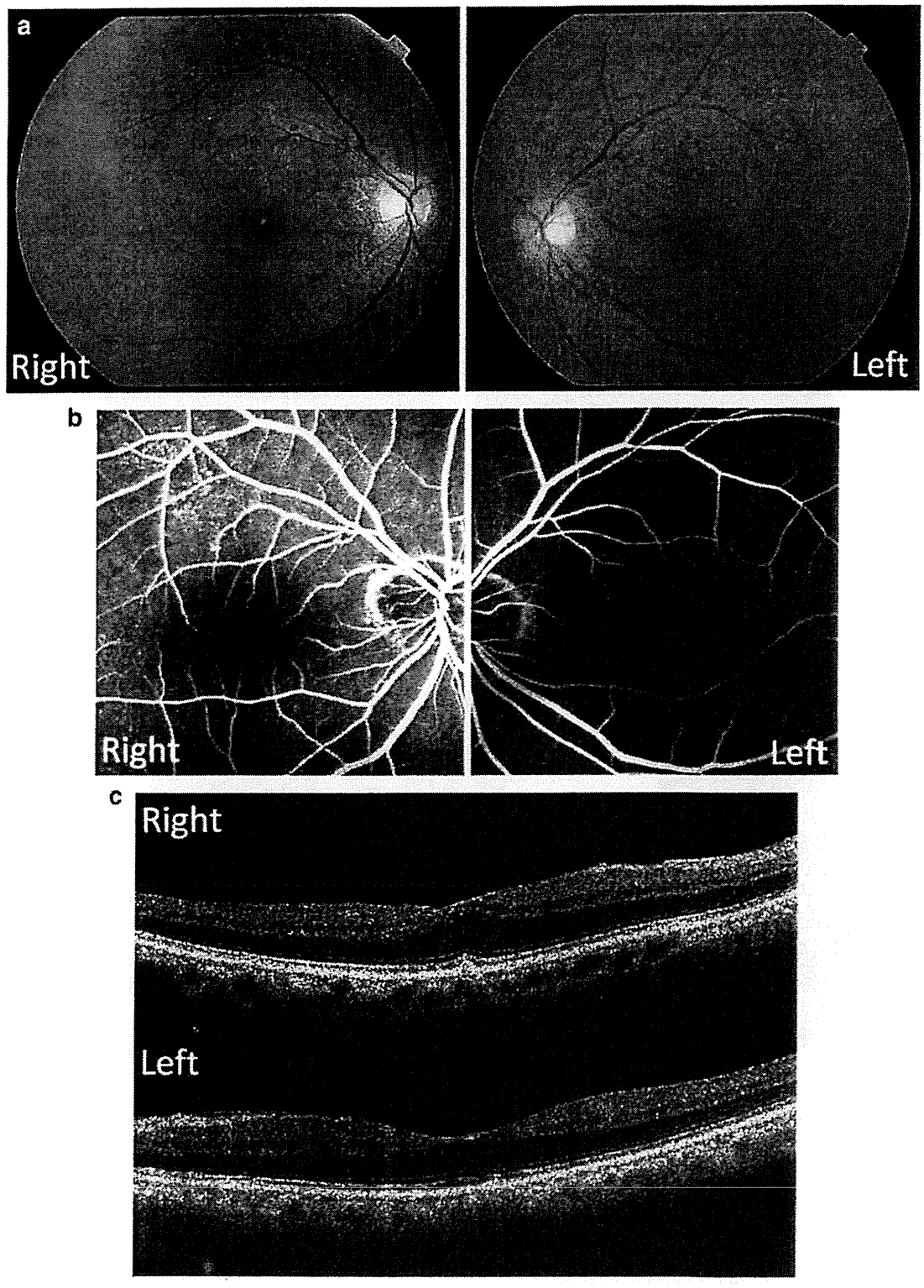

Fig. 1 Fundus photography, fluorescein angiography, and SD-OCT performed at the initial visit of the patient. **a** Fundus photographs revealed no abnormality in either eye. **b** Fundus fluorescence angiography revealed no abnormality in either eye. **c** Spectral domain-optical coherence tomography (SD-OCT) images for a 6-mm horizontal scan of the retina were essentially normal, with the exception of a slight irregularity of the retinal pigment epithelium in both eyes

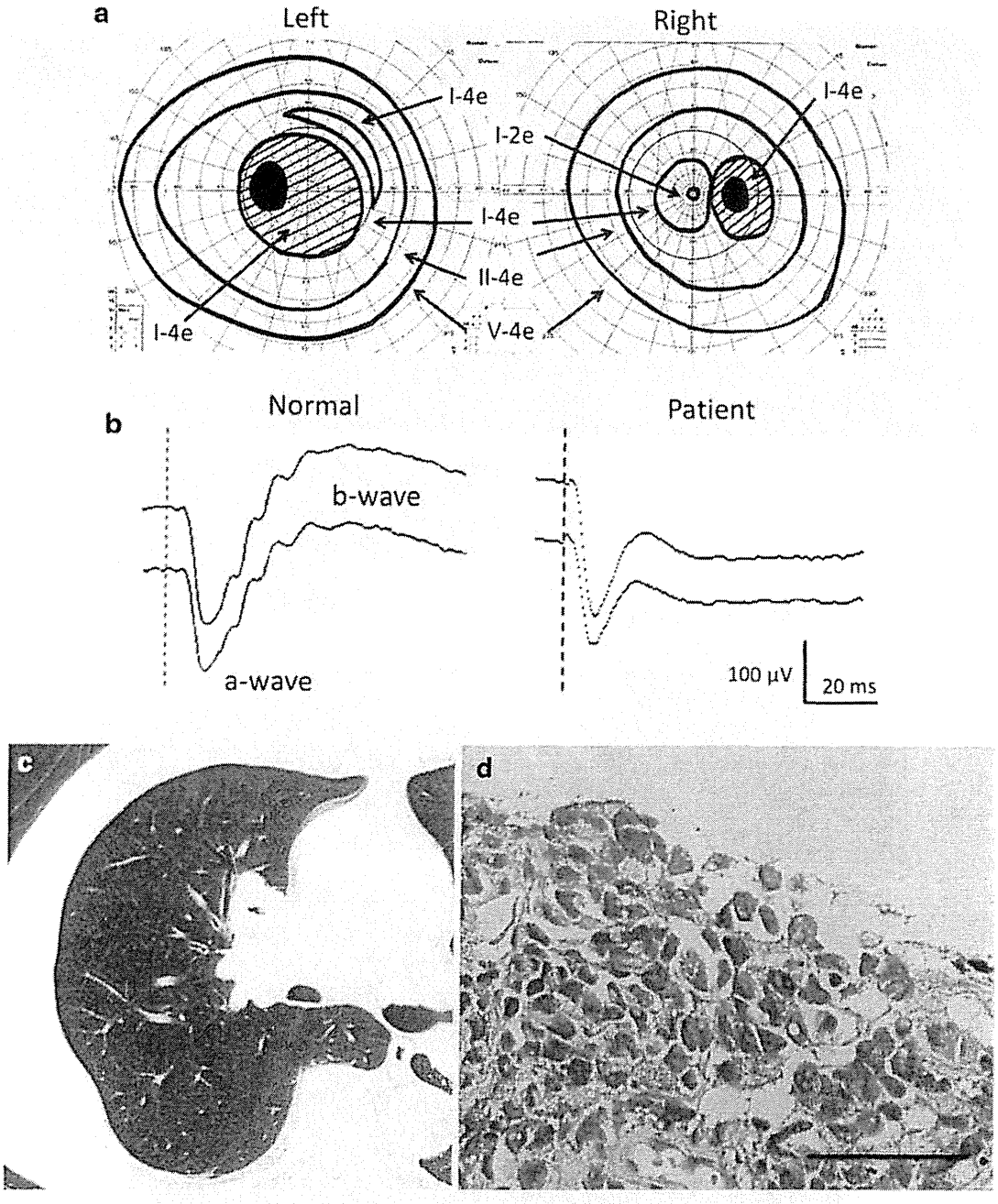

Fig. 2 Goldmann visual fields, full-field ERGs, CT of the right lung, and histology of a specimen obtained from the hilar lymph node of the patient. **a** Goldmann visual fields revealed a relative central scotoma including the blind spot OD and a relative scotoma around the blind spot OS. **b** Full-field electroretinograms (ERGs) with a bright flash stimulus after dark adaptation showed a "negative-type" pattern for the patient (*right*) compared with the normal pattern (*left*). **c** A computed tomography (CT) scan revealed a tumor in the right lung (*red arrow*). **d** Hematoxylin–eosin staining of a biopsy specimen obtained from a hilar lymph node in the right lung revealed spindle-shaped malignant cells. *Scale bar* 50 µm

TRPM1 is a component of the visual transduction cation channel specifically expressed in retinal ON bipolar cells [15–17, 19]. Immunohistology of the adult mouse retina revealed punctate TRPM1 signals at the tips of ON bipolar cell dendrites detected with antibodies to metabotropic glutamate receptor 6 (mGluR6) and to the α subunit of the G_o protein [16]. TRPM1-null mice were also shown to lack ON bipolar cell responses to light [15, 16]. In addition, *TRPM1* mutations have been associated with the complete form of congenital stationary night blindness (CSNB) in

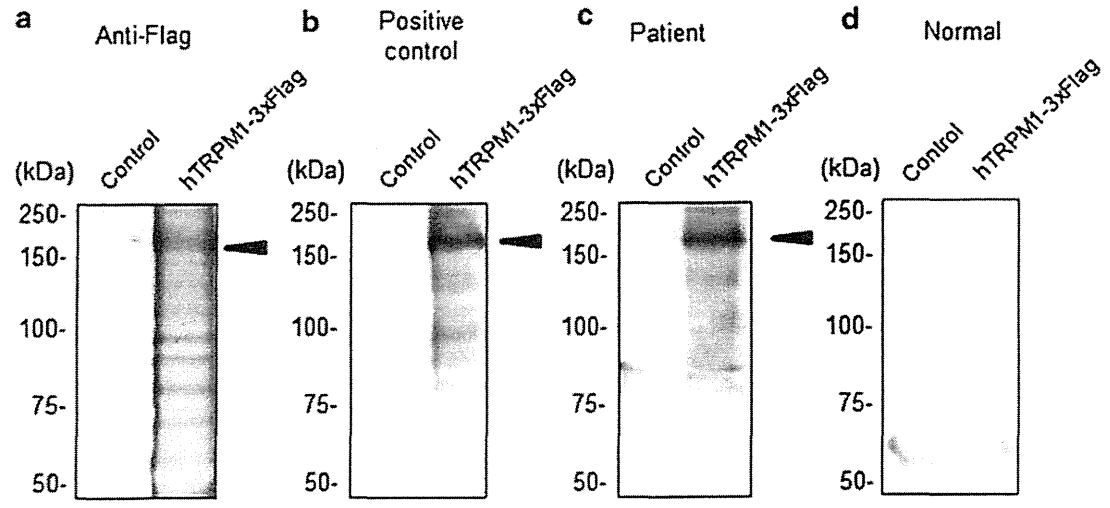

Fig. 3 Immunoblot analysis of serum from the patient for reactivity with TRPM1. HEK293T cells transfected with the expression vector pCAGGS alone (*control*) or with pCAGGS encoding human transient receptor potential cation channel, subfamily M, member 1 (*TRPM1*) tagged with three copies of the flag epitope were subjected to immunoblot analysis with antibodies to the flag tag (**a**), with serum from a patient previously shown to contain autoantibodies to TRPM1 as a positive control (**b**), with serum from the proband (**c**), and with normal control serum (**d**). *Arrowheads* indicate the 3× flag-tagged TRPM1 protein, which showed substantial reactivity with serum from the proband. The positions of molecular size standards (in kilodaltons) are also shown

humans, which is characterized by pronounced dysfunction of the retinal ON pathway [20–23]. These observations suggest that TRPM1 plays a key role in synaptic transmission from photoreceptors to ON bipolar cells. It is possible that ectopic expression of TRPM1 in the malignant melanoma cells of the patient triggered the production of autoantibodies to this protein by B lymphocytes. These antibodies might then have reacted with TRPM1 in retinal ON bipolar cells, resulting in severe dysfunction of the retinal ON pathway.

The average latency from the diagnosis of melanoma to that of MAR was previously found to be 3.6 years, with a range of 2 months–19 years [5]. We diagnosed the present patient with malignant melanoma after only 18 days from the time of his first visit. However, he died 11 months later as a result of metastasis to several organs. In the present case, the visual symptoms preceded the diagnosis of malignant melanoma. The patient complained of blurred vision, night blindness, and photopsia; but Fundus photographs, fluorescein angiograms, and SD-OCT findings were all essentially normal at his initial visit. Perimetry revealed relative scotomas OU. It was his "negative-type" ERGs, indicative of extensive bipolar cell dysfunction, that led us to suspect the patient might have MAR. We, therefore, recommend that ERGs be performed on patients with progressive visual disturbance of unknown origin.

"Negative-type" ERGs are also observed in patients with CSNB. A previous study [5] found that 18 of 27 patients with MAR showed either central or paracentral scotomas or depressions, and 6 of 27 patients had arcuate visual field defects. The present patient had relative central scotomas that included or surrounded the blind spot. In contrast, patients with CSNB manifest a largely intact visual field. MAR patients also show a greater loss of S (blue) cone sensitivity by perimetry than do CSNB patients, and S cone ERGs were not detected in MAR patients [2]. Two subtypes of CAR were previously identified [2]: one in which cone cells are damaged and in which Goldmann perimetry reveals central scotoma, and one in which rod cells are damaged and in which Goldmann perimetry reveals annular scotoma. We speculate that the visual field disturbance of the present patient reflected damage to cone cells.

Drug therapy for MAR is aimed at immunomodulation in order to attenuate the autoimmune attack on the retina before irreversible damage occurs. Treatments include corticosteroid administration, plasmapheresis, intravenous injection of immunoglobulin and immunosuppression. However, the effectiveness of these treatments remains unclear. Oral corticosteroid treatment alone was found to be beneficial in only one of seven patients [5]. In the present study, the patient was treated with oral prednisolone. We believe that this treatment was effective because the vitreous opacity and enlarged blind spots were markedly attenuated after its onset. Further studies are needed to determine the optimal treatment for MAR.

There are several limitations to our study. First, we recorded only bright-flash ERGs after dark adaptation; we did not record rod responses to low-intensity stimuli, photopic responses, or photopic ERGs in response to a

long-duration stimulus in order to determine whether the postreceptor ON pathway was specifically affected. Second, we did not perform immunohistochemical analysis with the serum of the patient to confirm that the autoantibodies recognize retinal bipolar cells. And third, we did not confirm that the autoantibodies actually reacted with malignant melanoma proteins.

In conclusion, we described a Japanese patient with MAR whose serum was positive for autoantibodies to TRPM1. Visual symptoms preceded the identification of malignant melanoma in this patient, and his "negative-type" ERGs led us to suspect a diagnosis of MAR. Further studies are warranted to determine both the proportion of MAR patients who develop TRPM1 autoantibodies as well as the best treatment option for this type of paraneoplastic retinopathy.

Acknowledgments We thank Mr. Takahisa Furukawa (Institute for Protein Research, Osaka University) for providing the expression vector for TRPM1 as well as Dr. Duco I. Hamasaki for editing the manuscript.

Conflicts of interest Y. Morita, None; K. Kimura, None; Y. Fujitsu, None; A. Enomoto, None; S. Ueno, None; M. Kondo, None; K. Sonoda, None.

References

1. Berson EL, Lessell S. Paraneoplastic night blindness with malignant melanoma. Am J Ophthalmol. 1988;106:307–11.
2. Milam AH, Saari JC, Jacobson SG, Lubinski WP, Feun LG, Alexander KR. Autoantibodies against retinal bipolar cells in cutaneous melanoma-associated retinopathy. Invest Ophthalmol Vis Sci. 1993;34:91–100.
3. Potter MJ, Thirkill CE, Dam OM, Lee AS, Milam AH. Clinical and immunocytochemical findings in a case of melanoma-associated retinopathy. Ophthalmology. 1999;106:2121–5.
4. Lei B, Bush RA, Milam AH, Sieving PA. Human melanoma-associated retinopathy (MAR) antibodies alter the retinal ON response of the monkey ERG in vivo. Invest Ophthalmol Vis Sci. 2000;41:262–6.
5. Keltner JL, Thirkill CE, Yip PT. Clinical and immunologic characteristics of melanoma-associated retinopathy syndrome: eleven new cases and a review of 51 previously published cases. J Neuroophthalmol. 2001;21:173–87.
6. Alexander KR, Barnes CS, Fishman GA, Milam AH. Nature of the cone ON pathway dysfunction in melanoma-associated retinopathy. Invest Ophthalmol Vis Sci. 2002;43:1189–97.
7. Chan JW. Paraneoplastic retinopathies and optic neuropathies. Surv Ophthalmol. 2003;48:12–38.
8. Adamus G. Autoantibody targets and their cancer relationship in the pathogenicity of paraneoplastic retinopathy. Autoimmun Rev. 2009;8:410–4.
9. Potter MJ, Adamus G, Szabo SM, Lee R, Mohaseb K, Behn D. Autoantibodies to transducin in a patient with melanoma-associated retinopathy. Am J Ophthalmol. 2002;134:128–30.
10. Hartmann TB, Bazhin AV, Schadendorf D, Eichmuller SB. SEREX identification of new tumor antigens linked to melanoma-associated retinopathy. Int J Cancer. 2005;114:88–93.
11. Lu Y, Jia L, He S, Hurley MC, Leys MJ, Jayasundera T, et al. Melanoma-associated retinopathy: a paraneoplastic autoimmune complication. Arch Ophthalmol. 2009;127:1572–80.
12. Bazhin AV, Dalke C, Willner N, Abschütz O, Wildberger HGH, Philippov PP, et al. Cancer-retina antigens as potential paraneoplastic antigens in melanoma-associated retinopathy. Int J Cancer. 2009;124:140–9.
13. Dhingra A, Fina ME, Neinstein A, Ramsey DJ, Xu Y, Fishman GA, et al. Autoantibodies in melanoma-associated retinopathy target TRPM1 cation channels of retinal ON bipolar cells. J Neurosci. 2011;31:3962–7.
14. Kondo M, Sanuki R, Ueno S, Nishizawa Y, Hashimoto N, Ohguro H, et al. Identification of autoantibodies against TRPM1 in patients with paraneoplastic retinopathy associated with ON bipolar cell dysfunction. PLoS One. 2011;6:e19911.
15. Morgans CW, Zhang J, Jeffrey BG, Nelson SM, Burke NS, Duvoisin RM, et al. TRPM1 is required for the depolarizing light response in retinal ON bipolar cells. Proc Natl Acad Sci USA. 2009;106:19174–8.
16. Koike C, Obara T, Uriu Y, Numata T, Sanuki R, Miyata K, et al. TRPM1 is a component of the retinal ON bipolar cell transduction channel in the mGluR6 cascade. Proc Natl Acad Sci USA. 2010;107:332–7.
17. Koike C, Numata T, Ueda H, Mori Y, Furukawa T. TRPM1: a vertebrate TRP channel responsible for retinal ON bipolar function. Cell Calcium. 2010;48:95–101.
18. Loduca AL, Zhang C, Zelkha R, Shahidi M. Thickness mapping of retinal layers by spectral-domain optical coherence tomography. Am J Ophthalmol. 2010;150:849–55.
19. Klooster J, Blokker J, Ten Brink JB, Unmehopa U, Fluiter K, Bergen AA. Ultrastructural localization and expression of TRPM1 in the human retina. Invest Ophthalmol Vis Sci. 2011;52:8356–62.
20. Li Z, Sergouniotis PI, Michaelides M, Mackay DS, Wright GA, Devery S, et al. Recessive mutations of the gene TRPM1 abrogate ON bipolar cell function and cause complete congenital stationary night blindness in humans. Am J Hum Genet. 2009;85:711–9.
21. van Genderen MM, Bijveld MM, Claassen YB, Florijn RJ, Pearring JN, Meire FM, et al. Mutations in TRPM1 are a common cause of complete congenital stationary night blindness. Am J Hum Genet. 2009;85:730–6.
22. Audo I, Kohl S, Leroy BP, Munier FL, Guillonneau X, Mohand-Saïd S, et al. TRPM1 is mutated in patients with autosomal-recessive complete congenital stationary night blindness. Am J Hum Genet. 2009;85:720–9.
23. Nakamura M, Sanuki R, Yasuma TR, Onishi A, Nishiguchi KM, Koike C, et al. TRPM1 mutations are associated with the complete form of congenital stationary night blindness. Mol Vis. 2010;16:425–37.

Clinical Ophthalmology Dove

CASE REPORT

Peripheral capillary nonperfusion and full-field electroretinographic changes in eyes with frosted branch-like appearance retinal vasculitis

Yoshitsugu Matsui
Hideyuki Tsukitome
Eriko Uchiyama
Yuko Wada
Tatsuya Yagi
Hisashi Matsubara
Mineo Kondo

Department of Ophthalmology, Mie University Graduate School of Medicine, Tsu, Japan

Abstract: We report a patient with frosted branch-like appearance retinal vasculitis associated with peripheral capillary nonperfusion and full-field electroretinographic changes. A 62-year-old man presented with sudden bilateral decreased vision accompanied by headaches. His best-corrected visual acuity was 0.01 in both eyes. Fundus examination and fluorescein angiography showed bilateral frosted branch-like appearance retinal vasculitis, and spectral-domain optical coherence tomography showed severe macular edema in both eyes. The cerebrospinal fluid analyses showed an increased lymphocyte count and protein levels. He was treated with systemic corticosteroid therapy, and his best-corrected visual acuity improved to 0.8 OD and 1.0 OS at 6 months after onset. However, fluorescein angiography showed a lack of capillary perfusion in the periphery, and the oscillatory potentials on full-field electroretinography were severely reduced in both eyes. These findings indicated extensive retinal ischemia and inner retinal dysfunction, and that fluorescein angiography and full-field electroretinograms can be useful during follow-up of eyes with frosted branch-like appearance retinal vasculitis.

Keywords: frosted branch angiitis, aseptic meningitis, optical coherence tomography, electroretinogram, oscillatory potentials

Introduction

Frosted branch angiitis[1] is a rare type of periphlebitis characterized by white sheathing of the retinal vessels in association with different types of inflammatory eye disease.[2–4] The onset of frosted branch angiitis is usually sudden, and patients may complain of painless blurred vision, a central blind area, floaters, and photopsias.

Most patients with frosted branch angiitis respond to systemic corticosteroid therapy with good recovery of visual acuity, but various adverse complications have also been reported. These complications include macular scarring, retinal vein or artery occlusion, macular epiretinal membrane formation, diffuse retinal fibrosis, optic disc atrophy, peripheral capillary nonperfusion, and vitreous hemorrhage, all of which have been reviewed elsewhere.[3]

We report our findings in a 62-year-old man with bilateral frosted branch-like appearance retinal vasculitis accompanied by aseptic meningitis. He was treated with systemic corticosteroid therapy with good recovery of visual acuity. However, examinations at 6 months after onset revealed peripheral capillary nonperfusion and severe reduction of the amplitudes of oscillatory potentials on the electroretinogram. These changes suggested extensive retinal ischemia and inner retinal dysfunction, which required photocoagulation.

Correspondence: Mineo Kondo
Department of Ophthalmology, Mie University Graduate School of Medicine, 2-175 Edobashi, Tsu, 514-8507, Japan
Tel +815 9231 5027
Fax +815 9231 3036
Email mineo@clin.medic.mie-u.ac.jp

Case report

A 62-year-old man presented with sudden bilateral decrease of vision accompanied by headaches. He did not have any systemic diseases, and his family history revealed no other members with eye disease. He had never experienced oral ulcers or skin lesions previously.

At our initial examination, his best-corrected visual acuity was 0.01 in both eyes, and Goldmann perimetry showed a severe central scotoma in both eyes. The intraocular pressure was 18 mmHg OD and 16 mmHg OS. Slit-lamp examination showed many fine keratic precipitates and cells in the aqueous and vitreous of both eyes. Severe sheathing of the retinal vessels and retinal hemorrhages was detected in both eyes by ophthalmoscopy (Figure 1, upper panel). Fluorescein angiography showed perivenous staining and leakage from the vessels (Figure 1, lower panel). Spectral-domain optical coherence tomography (Spectralis®, Heidelberg Engineering, Heidelberg, Germany) demonstrated severe macular edema with central macular thickness of 1045 μm OD and 991 μm OS (Figure 2, uppermost panel). We also recorded full-field electroretinograms and found that the amplitudes of the mixed rod and cone responses after dark adaptation were severely attenuated in both eyes (Figure 3, middle panel).

On systemic examination, blood count, biochemical analysis including kidney function tests, urine testing, and chest x-rays were within normal limits. Angiotensin-converting enzyme levels were also within normal limits. Tests for syphilis and human immunodeficiency virus were negative.

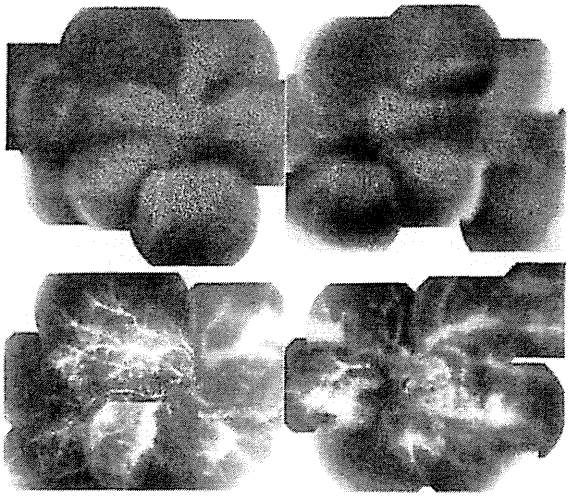

Figure 1 Fundus photographs and fluorescein angiograms at initial examination showing bilateral diffuse perivascular sheathing and retinal edema with intraretinal hemorrhages (upper panel).
Note: Fluorescein angiography shows extensive vascular leakage and retinal edema (lower panel).

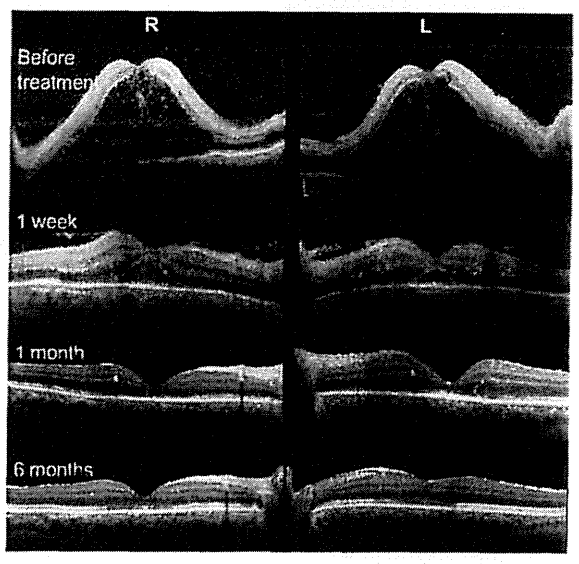

Figure 2 Changes in spectral-domain optical coherence tomograms at onset, and at one week, one month, and 6 months after treatment.

Lupus anticoagulant and anticardiolipin antibody were not detected. The HLA type was A11, A24, B39, B54, DR4, and DR8. Herpes simplex and varicella zoster IgG antibody titers suggested prior exposure only. Polymerase chain reaction analysis of the aqueous humor was negative for herpes simplex, herpes zoster, and cytomegalovirus DNA. Cerebrospinal fluid analysis disclosed an increased leukocyte count (72/mL, mononuclear cells) and protein level (49 mg/dL; normal 10–40 mg/dL). Cerebrospinal fluid cultures were negative.

Based on the results of these systemic examinations, we diagnosed our patient as having frosted branch-like appearance retinal vasculitis associated with aseptic meningitis. He was treated with pulsed steroid therapy (methylprednisolone 1000 mg/day × 3 days) followed by oral prednisolone (1 mg/kg/day), topical steroids, and mydriasis.

One month later, the patient's best-corrected visual acuity improved to 0.6 (OD) and 0.5 (OS), and spectral-domain optical coherence tomography showed a reduction in macular edema (Figure 2, third panel).

Six months after the start of steroid therapy, best-corrected visual acuity was improved to 0.8 OD and 1.0 OS and the fundus had returned to nearly normal (Figure 4, upper panel). Spectral-domain optical coherence tomography showed that the thickness of the retina was normal but the inner segment/outer segment junction of the photoreceptors was still disrupted at the fovea in both eyes (Figure 2, lowest panel). We performed fluorescein angiography again, and found that there were extensive areas without capillary perfusion in the

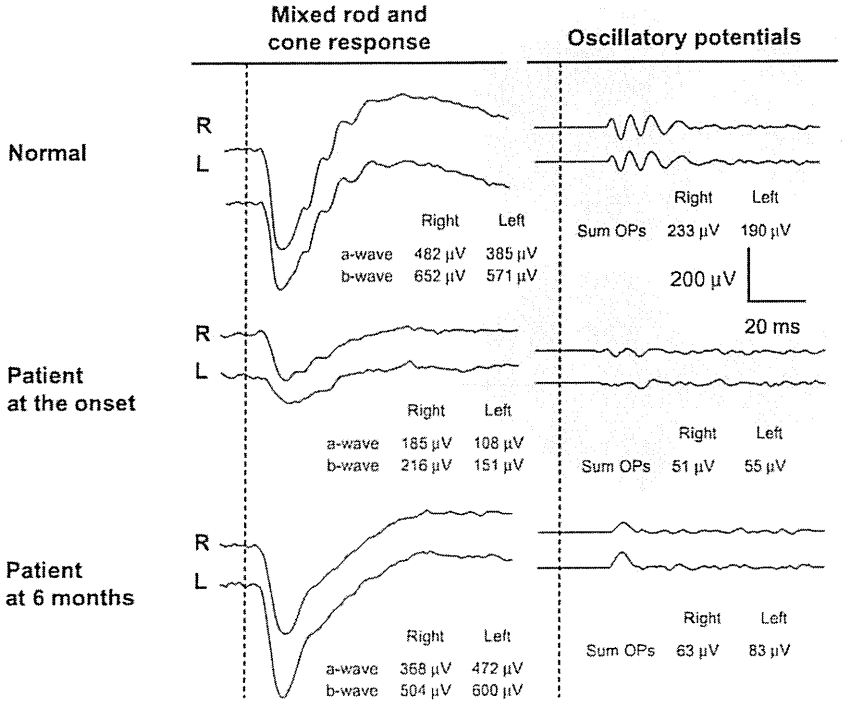

Figure 3 Changes in full-field electroretinograms.
Notes: Full-field mixed rod and cone electroretinograms were recorded after 20 minutes of dark adaptation at onset and 6 months after treatment. Full-field electroretinograms were elicited by a contact lens electrode with a built-in white light emitting diode (LE-2000, Tomey Co, Nagoya, Japan).[11] The stimulus intensity was 10.0 cd-s/m^2 (photopic units). Although the a-waves and b-waves recovered to normal, the oscillatory potentials were still severely reduced at 6 months after onset.

periphery of both eyes (Figure 4, lower panel). Full-field electroretinograms demonstrated nearly normal a waves and b waves, but severely reduced oscillatory potentials in both eyes (Figure 3, lowest panel). These results suggested extensive retinal ischemia and inner retinal dysfunction.

We then performed photocoagulation of the peripheral retina to prevent neovascularization and vitreous hemorrhage. There were no retinal complications in our patient during one year of follow-up after photocoagulation.

Discussion

Frosted branch angiitis is considered to be a clinical subtype of diffuse retinal periphlebitis and is associated with various types of systemic and ocular disease.[2–4] Frosted branch angiitis is reported to be associated with virus and bacterial infections, lymphoma, leukemia, Crohn's disease, systemic lupus, toxoplasmosis, Behçet's disease, central retinal vein occlusion, nephritis, and other systemic diseases.[2–4] The frosted branch-like appearance retinal vasculitis in our patient was believed to be associated with aseptic meningitis because he had headaches and an increased lymphocyte count and protein level in his cerebrospinal fluid. Further, no viral infection could be detected.

Johkura et al[5] reported a 20-year-old woman with frosted branch angiitis and aseptic meningitis who had headaches, nausea, and vomiting, and cerebrospinal fluid study showed lymphocyte counts increased to 83/mL and a protein level of 42 mg/dL. More recently, Chaume et al[6] reported an 11-year-old boy with frosted branch angiitis and aseptic meningitis. Their clinical findings and laboratory data were very similar to those in our patient.

In our patient, fluorescein angiography showed extensive areas without capillary perfusion in the peripheral retina and a selective reduction in amplitudes of the oscillatory potentials in both eyes. It is widely accepted that oscillatory potentials originate mainly from inhibitory neural pathways in the inner retina, including those of the amacrine and ganglion cells.[7] It has also been reported that a selective reduction in the amplitude of oscillatory potentials is also found when inner retinal function is extensively impaired, eg, in diabetic retinopathy or central retinal vein occlusion.[7] Thus, the findings of a lack of peripheral capillary perfusion and selective loss of oscillatory potentials on the electroretinogram in our patient strongly suggest that the retina was extensively ischemic and required photocoagulation. Luo et al[8] also used full-field electroretinograms during follow-up of a

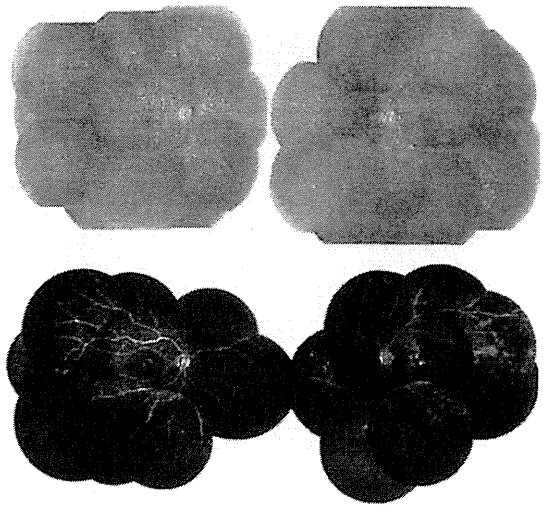

Figure 4 Fundus photographs and fluorescein angiograms 6 months after treatment.
Note: The fundus had recovered to nearly normal, but the fluorescein angiograms show extensive lack of capillary perfusion in the peripheral retina (lower panel).

5-year-boy with frosted branch angiitis, but reported that all electroretinographic components recovered to normal 6 months after treatment.

Our search using PubMed and the Japan Medical Abstracts Society yielded only three papers on frosted branch angiitis associated with peripheral capillary nonperfusion. In 1988, Kleiner et al[2] reported a 25-year-old man with frosted branch angiitis who developed multiple branch vein occlusion, capillary nonperfusion, and retinal neovascularization. In 1989, Terasaki et al[9] reported on a 21-year-old woman with frosted branch angiitis, who developed peripheral capillary nonperfusion and retinal neovascularization which required panretinal photocoagulation 18 months after onset. In 1993, Harigai et al[10] reported on a 39-year-old man with frosted branch angiitis who developed peripheral capillary nonperfusion at 7 months after onset. Despite panretinal photocoagulation, vitreous hemorrhages developed in his right eye. Although fluorescein angiography was repeatedly performed during follow-up, full-field electroretinograms were not recorded in these three patients.

The findings in our case suggest that extensive retinal ischemia and inner retinal dysfunction can occur in eyes with frosted branch-like appearance retinal vasculitis, and careful follow-up examinations are needed, even after good recovery of visual acuity. In addition to fluorescein angiography, full-field electroretinography may be useful during follow-up of these patients.

Acknowledgments

Funding for this work was received from the Ministry of Education, Culture, Science and Technology (23592603), Japan. The authors thank Duco I Hamasaki for editing the manuscript.

Disclosure

The authors report that they have no competing interests in this work.

References

1. Ito Y, Nakano M, Kyu N, Takeuchi M. Frosted branch angiitis in a child. *Rinsho Ganka*. 1976;30(7):797–803. Japanese.
2. Kleiner RC, Kaplan HJ, Shakin JL, Yannuzzi LA, Crosswell HH Jr, McLean WC Jr. Acute frosted retinal periphlebitis. *Am J Ophthalmol*. 1998;106(1):27–34.
3. Walker S, Iguchi A, Jones NP. Frosted branch angiitis: a review. *Eye (Lond)*. 2004;18(5):527–533.
4. Kleiner RC. Frosted branch angiitis: clinical syndrome or clinical sign? *Retina*. 1997;17(5):370–371.
5. Johkura K, Hara A, Hattori T, Hasegawa O, Kuroiwa Y. Frosted branch angitis associated with aseptic meningitis. *Eur J Neurol*. 2000;7(2):241.
6. Chaume A, Lemelle I, Chastagner P, Angioi K. A case report of frosted branch angiitis associated with aseptic meningitis in a young boy. *J Fr Ophtalmol*. 2011;34(2):129. e1–e5. French.
7. Wachtmeister L. Oscillatory potentials in the retina: what do they reveal. *Prog Retin Eye Res*. 1998;17(4):485–521.
8. Luo G, Yang P, Huang S, Jiang F, Wen F. A case report of frosted branch angiitis and its visual electrophysiology. *Doc Ophthalmol*. 1998–1999;97(2):135–142.
9. Terasaki H, Yanagida K, Tanaka T. An adult case of frosted branch angiitis with various systemic manifestation. *Folia Ophthalmol Jpn*. 1989;40(11):2438–2442. Japanese.
10. Harigai R, Seki R, Emi K, Oguro Y, Sato Y. A case of frosted branch angiitis associated with vitreous hemorrhage. *Folia Ophthalmol Jpn*. 1993;44(6):772–778. Japanese.
11. Kondo M, Piao CH, Tanikawa A, Horiguchi M, Miyake Y. A contact lens electrode with built-in high intensity white light-emitting diodes. *Doc Ophthalmol*. 2001;102(1):1–9.

Jpn J Ophthalmol (2014) 58:232–236
DOI 10.1007/s10384-014-0316-6

THE OFFICIAL INTERNATIONAL JOURNAL OF THE JAPANESE OPHTHALMOLOGICAL SOCIETY

CLINICAL INVESTIGATION

Electroretinograms and level of aqueous vascular endothelial growth factor in eyes with hemicentral retinal vein occlusion or branch retinal vein occlusion

Shunsuke Yasuda · Shu Kachi · Shinji Ueno · Hiroaki Ushida · Chang-Hua Piao · Mineo Kondo · Hiroko Terasaki

Received: 14 August 2013 / Accepted: 14 February 2014 / Published online: 26 March 2014

Abstract
Purpose Hemicentral retinal vein occlusion (hCRVO) is a disease related to CRVO but not to branch retinal vein occlusion (BRVO). We reported a significant correlation between aqueous vascular endothelial growth factor (VEGF) levels and the implicit time of 30-Hz flicker electroretinogram (ERG) in CRVO eyes. The purpose of this study was to compare aqueous VEGF levels and ERG components between hCRVO and BRVO eyes.
Methods The medical records of patients with macular edema secondary to hCRVO (12 eyes) or BRVO (16 eyes) and received an intravitreal injection of bevacizumab (IVB) at the Nagoya University Hospital from July 2009 to May 2013 were reviewed. Full-field ERGs were recorded before the IVB. Aqueous humor was collected just before the IVB to measure VEGF concentration. Differences in aqueous VEGF level and ERG components between hCRVO and BRVO eyes were determined.
Results Mean aqueous VEGF concentration in hCRVO eyes was significantly higher than that in BRVO eyes (504 vs. 148 pg/ml, $P < 0.05$). The implicit time of 30-Hz flicker ERG was significantly longer in hCRVO than in BRVO eyes (33.5 vs. 29.8 ms, $P < 0.01$).
Conclusion The significant difference in VEGF levels in aqueous and implicit times of 30-Hz flicker ERG suggest that retinal ischemia is more manifest in hCRVO than in BRVO eyes.

S. Yasuda · S. Kachi (✉) · S. Ueno · H. Ushida · C.-H. Piao · M. Kondo · H. Terasaki
Department of Ophthalmology, Nagoya University Graduate School of Medicine, 65 Tsuruma-cho, Showa-ku, Nagoya 466-8550, Japan
e-mail: kachishu-ngy@umin.ac.jp

Keywords Hemicentral retinal vein occlusion · Branch retinal vein occlusion · Electroretinogram · Vascular endothelial growth factor

Introduction

Hemicentral retinal vein occlusion (hCRVO) is a disease related to CRVO but not to branch retinal vein occlusion (BRVO). It is reported that in a certain proportion of human eyes, a two-trunked central retinal vein (CRV) may persist in the anterior part of the optic nerve as a congenital anomaly. One of the two trunks may be occluded in the optic nerve to produce hCRVO. On the other hand, BRVO typically occurs at an arteriovenous crossing [1, 2]. CRVO instigates retinal ischemia, which induces up-regulation of vascular endothelial growth factor (VEGF), which leads to iris neovascularization [3–7]. Similar changes occur in eyes with hCRVO but not in eyes with BRVO. It is reported that VEGF levels in the vitreous were significantly higher in eyes with CRVO and hCRVO than in eyes with BRVO [8]. Results of several studies demonstrate that different components of full-field electroretinograms (ERGs) can be helpful in distinguishing ischemic from nonischemic CRVO [9–26]. We showed that implicit times of 30-Hz flicker ERG were significantly correlated with ocular VEGF level in CRVO eyes [27], and Noma et al. [28] report that they were significantly correlated with ocular VEGF level in BRVO eyes. However, little is known about the comparison of ERG parameters and ocular VEGF concentrations between hCRVO and BRVO eyes. The purpose of this study was to determine whether there are any differences in VEGF levels in the aqueous and in amplitudes and implicit times of different ERG components between hCRVO and BRVO eyes.

Patients and methods

The procedures used in this study conformed to the tenets of the World Medical Association's Declaration of Helsinki. The intravitreal injection of bevacizumab (IVB), collection of aqueous humor, and VEGF measurements were performed after obtaining approval of Nagoya University Hospital Ethics Review Board and a written informed consent from each patient.

Patients

We reviewed medical records of patients with macular edema secondary to hCRVO or BRVO and who received an IVB at the Nagoya University Hospital from July 2009 to May 2013. Patients with diabetic retinopathy were excluded.

Electroretinograms

Full-field ERGs, elicited by stimuli from a Ganzfeld dome, were recorded before IVB with a Burian–Allen bipolar contact lens electrode. The eyes were dark adapted for 30 min, and a rod response was elicited by blue light at an intensity of 5.2×10^3 cd/s/m^2. A mixed cone–rod ERG was elicited by a white flash of 44.2 cd/s/m^2, and cone ERGs and 30-Hz flicker ERGs were elicited by white stimuli of 4 and 0.9 cd/s/m^2, respectively. Cone and flicker ERGs were elicited by stimuli on a white background of 68 cd/m^2 [27].

Intravitreal injection of bevacizumab and collection of aqueous humor

The eyes were anesthetized with topical 1 % tetracaine, and the fornices were irrigated with 10 % povidone–iodine. A mean volume of 0.1 ml of aqueous humor was collected by anterior-chamber paracentesis with a 27-gauge needle attached to a 1-ml syringe. Each patient then received an intravitreal injection of 1.25 mg/0.05 ml bevacizumab using a 30-gauge needle inserted through the sclera 3.5 mm from the limbus. Antibiotics drops were given for 3 days after the injection [27].

Measurement of VEGF level in aqueous by ELISA

Aqueous samples were stored at −80 °C until use. VEGF concentration was measured using enzyme-linked immunosorbent assay (ELISA) using a commercially available kit (Quantikine; R&D Systems, Minneapolis, MN, USA), which measures human VEGF121 and VEGF165 [27].

Statistical analyses

The significance of differences in VEGF levels of aqueous humor and ERG parameters between hCRVO and BRVO eyes was determined with the Mann–Whitney U test. Commercially available software (SPSS v. 17.0J for Windows; SPSS Inc., Chicago, IL, USA) was used for all statistical analyses. $P < 0.05$ was considered significant.

Results

Patients

Demographics of the patients with hCRVO and BRVO are shown in Table 1. Twenty-eight eyes of 28 patients with macular edema secondary to hCRVO ($n = 12$) and BRVO ($n = 16$) were studied. There were nine men and three women in the hCRVO group and nine men and seven women in the BRVO group. Mean age was 66.9 years in the hCRVO group and 61.6 years in the BRVO group. Mean visual acuity before IVB was 0.69 logarithm of the minimum angle of resolution (logMAR) units in the hCRVO group and 0.45 logMAR units in the BRVO group. Mean duration of symptoms before IVB was 15.6 weeks in the hCRVO group and 14.3 weeks in the BRVO group.

Fluorescein angiography showed that eight patients with hCRVO and four with BRVO had a nonperfusion area (NPA), although none of the NPA was >10 DA (disc area) in size. Photocoagulation was applied to the NPA of these patients after IVB. There was no angle or iris neovascularization in any patient.

Comparison of ERG components between hCRVO and BRVO eyes

Rod, cone, single bright flash, and 30-Hz flicker ERG amplitudes of hCRVO group and BRVO group eyes are shown in Table 2; implicit times of the same parameters are shown in Table 3. Implicit times of 30-Hz flicker ERG of hCRVO eyes were significantly longer than that of BRVO eyes (33.5 ± 3.5 vs. 29.8 ± 2.0 ms; $P = 0.006$). There were no significant differences in the other ERG components.

Table 1 Characteristics of 28 patients with hemicentral retinal vein occlusion (hCRVO) and branch retinal vein occlusion (BRVO)

	hCRVO	BRVO	P value
Eyes	12	16	
Age[a]	66.9 ± 6.4	61.6 ± 9.8	0.12*
Sex (men/women)	9/3	9/7	0.31**
Visual acuity (logMAR)[a]	0.69 ± 0.49	0.45 ± 0.27	0.25*
Duration before treatment (weeks)[a]	15.6 ± 4.1	14.3 ± 5.1	0.68*

* Mann–Whitney U test, ** χ^2 test

[a] Data are the means ± standard deviation

Table 2 Comparison of amplitudes of ERGs between hemicentral retinal vein occlusion (hCRVO) and branch retinal vein occlusion (BRVO) eyes

ERG components	hCRVO eyes (average ± SD) μV[a]	BRVO eyes (average ± SD) μV[a]	*P* value*	Normal control eyes (average ± SD) μV[a]
Rod b-wave	73.5 ± 44.5	74.0 ± 24.7	0.88	101 ± 37.7
Single flash a-wave	294 ± 75.4	298 ± 97.6	0.96	383 ± 87.4
Single flash b-wave	419 ± 103	400 ± 108	0.50	535 ± 123
Single flash b/a ratio	1.37 ± 0.32	1.46 ± 0.22	0.40	1.40 ± 0.19
Cone a-wave	22.0 ± 5.5	28.3 ± 9.5	0.09	38.0 ± 11.9
Cone b-wave	58.7 ± 22.6	72.1 ± 26.5	0.05	94.6 ± 42.2
30-Hz flicker	22.0 ± 8.6	25.9 ± 16.1	0.69	28.1 ± 12.1

SD standard deviation

* Mann–Whitney *U* test

[a] Except for the single-flash b/a ratio

Table 3 Comparison of implicit times of ERGs between hemicentral retinal vein occlusion (hCRVO) and branch retinal vein occlusion (BRVO) eyes

ERG components	hCRVO eyes (average ± SD) ms	BRVO eyes (average ± SD) ms	*P* value*	Normal control eyes (average ± SD) ms
Single flash a-wave	13.9 ± 1.8	13.1 ± 0.7	0.23	12.6 ± 1.0
Single flash b-wave	55.6 ± 3.0	53.2 ± 3.4	0.06	52.0 ± 3.1
Cone a-wave	17.3 ± 2.2	16.5 ± 0.9	0.47	16.2 ± 0.77
Cone b-wave	33.8 ± 2.6	31.8 ± 1.9	0.06	30.3 ± 1.42
30-Hz flicker	33.5 ± 3.5	29.8 ± 2.0	0.006	28.8 ± 2.1

SD standard deviation

* Mann–Whitney *U* test

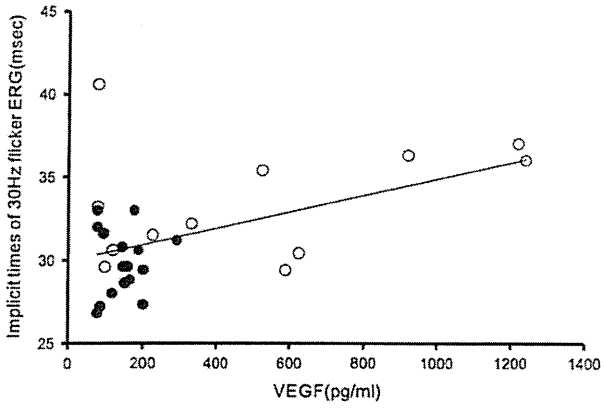

Fig. 1 Relationship between implicit times of 30-Hz flicker electroretinograms (ERGs) and aqueous vascular endothelial growth factor (VEGF) concentration in all 28 eyes. *Shaded circles* indicate branch retinal vein occlusion (BRVO) eyes, and *circles* indicate hemicentral retinal vein occlusion (hCRVO) eyes

Comparison of aqueous VEGF concentrations between hCRVO and BRVO eyes

Before the IVB, the mean aqueous VEGF concentration in hCRVO eyes was significantly higher than that in BRVO eyes (504 ± 429 vs. 148 ± 58 pg/ml, $P = 0.04$).

Relationship between implicit time of 30-Hz flicker ERGs and VEGF concentration in aqueous humor

Coefficients of correlation between the implicit time of the 30-Hz flicker ERGs and the VEGF concentration in aqueous humor were determined by Pearson product-moment correlation coefficient. The implicit times of 30-Hz flicker ERG were significantly correlated with the VEGF concentration in the aqueous in all 28 eyes ($P = 0.01$; $r = 0.50$). However, a significant correlation was not obtained when analysis was performed separately, either on BRVO eyes or hCRVO eyes (Fig. 1).

Discussion

Our results show that aqueous VEGF concentration was higher and the implicit time of 30-Hz flicker ERG was longer in hCRVO than in BRVO eyes. VEGF level in aqueous humor was consistent with that in the vitreous, as reported by Koss et al. [8]. Those authors found that mean VEGF concentrations in the vitreous were 162 pg/ml in BRVO eyes, 278 pg/ml in hCRVO eyes, and 212 pg/ml in CRVO eyes. Our results show that mean VEGF concentration in aqueous humor was 148 pg/ml in BRVO eyes and 504 pg/ml in hCRVO eyes. In addition, we previously